Food & Function

Accepted Manuscript

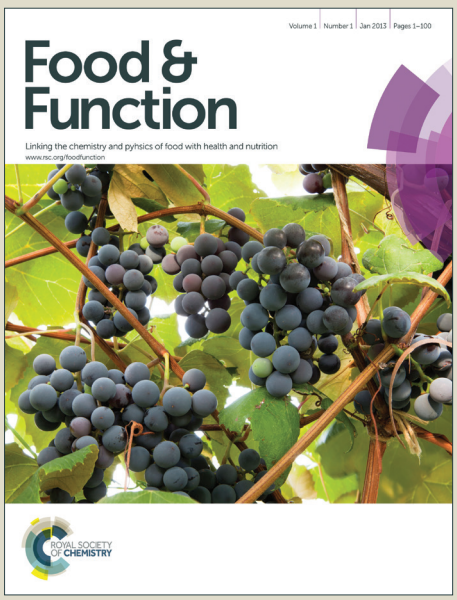

This is an *Accepted Manuscript*, which has been through the Royal Society of Chemistry peer review process and has been accepted for publication.

Accepted Manuscripts are published online shortly after acceptance, before technical editing, formatting and proof reading. Using this free service, authors can make their results available to the community, in citable form, before we publish the edited article. We will replace this *Accepted Manuscript* with the edited and formatted *Advance Article* as soon as it is available.

You can find more information about *Accepted Manuscripts* in the Information for Authors.

Please note that technical editing may introduce minor changes to the text and/or graphics, which may alter content. The journal's standard Terms & Conditions and the Ethical guidelines still apply. In no event shall the Royal Society of Chemistry be held responsible for any errors or omissions in this *Accepted Manuscript* or any consequences arising from the use of any information it contains.

ROYAL SOCIETY OF CHEMISTRY

www.rsc.org/foodfunction

Differences and Similarities in hepatic lipogenesis, gluconeogenesis and oxidative imbalance in mice fed diets rich in fructose or sucrose

Alini Schultz,

Sandra Barbosa-da-Silva,

Marcia B. Aguila,

Carlos A. Mandarim-de-Lacerda[1]

Laboratory of Morphometry, Metabolism, and Cardiovascular Disease, Biomedical Center, Institute of Biology, State University of Rio de Janeiro, RJ, Brazil

[1] Corresponding author: Laboratório de Morfometria e Morfologia Cardiovascular, Centro Biomedico, Instituto de Biologia, Universidade do Estado do Rio de Janeiro. AV. 28 de Setembro 87 (fds) 20551-030 Rio de Janeiro, RJ, Brasil. Phone: (+55.21) 2868.8316; Fax: 2868.8033. E-mail: mandarim@uerj.br; URL: www.lmmc.uerj.br.

Abstract

Changes in feeding habits are the primary environmental factor (though modifiable) commonly correlated with increases diseases such as obesity and associated comorbidities. Diets rich in fructose and sucrose have been related to the epidemic of obesity. Three groups of mice were studied during 15 weeks of consuming standard chow (SC), a high-fructose diet (HFru) and a high-sucrose diet (HSu). The animals did not present significant differences in food intake, energy intake, or body mass evolution at the end of the experiment. Although the findings in the HFru and HSu animals were not equal in magnitude, in comparison with the SC mice, the HFru and HSu animals showed hyperglycemia, hyperinsulinemia and hyperleptinemia as well as high levels of inflammatory adipokines, low adiponectin, and at high levels of total cholesterol, triacylglycerol, and liver enzymes. The liver of HFru (more) and HSu (less) groups showed fatty infiltration and areas of necroinflammation, which are characteristics of the transition from nonalcoholic fatty liver disease to nonalcoholic steatohepatitis. In addition, the HFru and HSu groups showed increased lipogenesis, gluconeogenesis, reduced beta-oxidation and antioxidant imbalance compared with the SC animals. In conclusion, current findings demonstrate comparable adverse effects on carbohydrate metabolism, inflammatory profile, antioxidant imbalance and NAFLD in the mice of the C57BL/6 strain fed a diet rich in sucrose or rich in fructose.

Keywords: Fructose; Sucrose; Insulin Resistance, Nonalcoholic fatty liver disease; Nonalcoholic steatohepatitis; Mice.

Introduction

Poor eating habits, especially the consumption of simple carbohydrates such as fructose and sucrose, represent an environmental factor, but modifiable, which is correlated with the development of various diseases, including obesity, insulin resistance (IR)/type II diabetes. Sucrose, the central component of *junk foods*, is a disaccharide composed of fructose and glucose, whose effects on the lipid profile, obesity and hyperglycemia have been studied.[1] Fructose is a monosaccharide that is abundant in fruits but has recently been used to sweeten processed products such as soft drinks and juices, in the form of high-fructose corn syrup.[2, 3]

The mechanism by which fructose is metabolized differs from that of sucrose. After fructose is absorbed from the intestine, it is metabolized in the liver directly, thus being independent of insulin. In the liver, fructose has two destinations: transformation into glucose and stored as glycogen, or being used as an energy source by hepatocytes. Thus, with the exception of fasting, when glycogen stores are low, all of the excess fructose will be converted to fat. It has been suggested that fructose exerts toxic effects on the liver similar to alcohol,[4] considering that alcohol is derived from the fermentation of sugar.

Sucrose is rapidly absorbed by the tissues and requires a high insulin release. For both fructose and sucrose, excess consumption is associated with obesity and visceral fat accumulation, which in turns increases the production of reactive oxygen species (ROS) and inflammatory cytokines.[5]

The antioxidant imbalance by the increased production of ROS and the reduction of antioxidant enzymes (glutathione system: oxidized (GSH), reduced (GSSH), peroxidase (GPx), reductase (GRx), catalase (Cat), and superoxide dismutase (SOD)) is an essential step in the presence of the inflammatory response in the liver.[6, 7]

In the liver, fructose is preferably metabolized into lipids contrarily to glucose. In addition, IR contributes to the presence of the intra-hepatic fat by signaling for *de novo lipogenesis*, resulting in nonalcoholic fatty liver disease – NAFLD,[8] and NAFLD evolution may reach nonalcoholic steatohepatitis (NASH), cirrhosis and hepatocarcinoma.[9]

The peroxisome proliferator-activated receptor (PPAR) is a family of transcription factors linked to carbohydrate, protein, and lipid metabolism as well as on cellular proliferation.

PPAR-alpha regulates the expression of genes involved in beta-oxidation in liver and muscle. PPAR-gamma is activated by fatty acids and their derivatives, and is related to IR and adipogenesis. The ratio PPAR-alpha / PPAR-gamma is a balance of the oxidation and fatty acid synthesis in the liver. [10]

However, the impact and magnitude of the effects of consuming isoenergetic diets rich in fructose and sucrose are still uncertain. The aim of the study was to investigate the effects of independent high intake of fructose and sucrose on body mass evolution and hepatic insult, altering lipogenesis, gluconeogenesis, beta-oxidation, inflammatory markers, and the hepatic oxidative balance.

Materials and methods

Animals and diets

The local ethics committee approved the animal care. The animals were bred in boxes under appropriate conditions of temperature (21±2° C) and humidity (60±10 %) with free access to food, water. The environment was subjected to 12 h light-dark cycles, according to the Guide for Care and Use of Laboratory Animals published by the U.S. National Institutes of Health (NIH Publication No. 85-23 revised in 1985).

Thirty C57BL6/J male mice at 12 weeks of age were randomly divided into three groups in accordance with the diet consumed and were monitored for 15 weeks. The diets were prepared following the AIN93 M guidelines, as seen in Table 1.[11]

a) Standard chow, SC (76 % carbohydrates - source: corn starch);
b) High-fructose diet, HFru (50 % fructose);
c) High-sucrose diet, HSu (50 % sucrose).

Body mass and food intake

Body mass (BM) was measured weekly during the experiment. In addition, the fresh chow was provided daily, and any remaining chow from the previous day was discarded. The food consumption of the mice during the preceding 72 h was measured using Compulse v 2.7.13 software (Harvard/Panlab, Barcelona, Spain). Moreover, food consumption was measured daily by calculating the amount of food supplied and the quantity of food remaining in the grid throughout the experiment. The product of the food consumption and the energy content of the diet was considered as the energy intake.

Euthanasia

The animals were fasted for 6 h on the day of sacrifice. Then, they were deeply anesthetized (intraperitoneal sodium pentobarbital, 150 mg/kg) and blood samples were obtained quickly via cardiac puncture.

The liver was dissected, and fragments from all hepatic lobes were either fixed in fresh prepared fixative (formaldehyde 4 % w/v in 0.1 M phosphate buffer, pH 7.2) for 48 h for light microscopy, or stored at -80° C for molecular studies. The fat pads were carefully dissected and weighed. The intra-abdominal fat pads (epididymal and retroperitoneal fat pads) and the subcutaneous fat (inguinal fat) were used to calculate the ratio: intra-abdominal fat/ subcutaneous fat (ratio IAF/SF).

Plasma analyses

Plasma was separated via centrifugation (120 g for 15 min) at room temperature. Total cholesterol, triacylglycerol, glucose, aminotransferase alanine (ALT) and aspartate aminotransferase (AST) were measured using a semiautomatic spectrophotometer and appropriate commercial kits (Bioclin, Quibasa, Belo Horizonte, MG, Brazil). The plasma concentrations of insulin, adiponectin, leptin, resistin, interleukin (IL)-6, and monocyte chemotactic protein (MCP)-1 were obtained using a multiplex ELISA kit (MADPK-71K-01, Millipore, Missouri, USA). IR was estimated through homeostasis model assessment: HOMA-IR = [(glucose x insulin)/22.5].[12]

Liver

Formalin-fixed liver specimens were embedded in Paraplast, and 5-µm-thick sections were stained with hematoxylin and eosin. Digital images were acquired at random in a blinded manner (Leica microscope, Wetzlar, Germany, and Lumenera Infinity 1-5c camera, Ottawa, Canada). Fifteen digital images per animal were studied to assess the volume density of liver steatosis by point counting as previously described.[13, 14]

Western Blotting

An approximately 120 mg liver sample was homogenized in lysis buffer (pH 6.4) containing protease and phosphatase inhibitors. The protein concentration was measured with the BCA Protein kit (Thermo Scientific, Rockford, IL). Thirty micrograms of liver protein were separated via electrophoresis on a polyacrylamide gel (SDS-PAGE) and transferred to a PVDF membrane (GE Healthcare Biosciences). The membranes were blocked with 5 % non-fat dry milk in Tris-buffered saline (TBS) (Amersham Biosciences, Uppsala, Sweden) containing 0.05 % Tween-20 (T-TBS) (Bio-Rad, CA, USA) and then incubated overnight at 4° C with antibodies to reveal the expression of the following proteins: sterol regulatory element-binding proteins (SREBP- 1c, Santa Cruz Biotechnology, code sc-367, CA, USA), carbohydrate-responsive element-binding protein (ChREBP, Santa Cruz Biotechnology, code sc-33764, CA, USA), the peroxisome proliferator-activated receptors PPAR-gamma (Santa Cruz Biotechnology, code sc-7273) and PPAR-alpha (Santa Cruz Biotechnology, code sc-9000, CA, USA), the glucose transporter (GLUT-2; Millipore, cat # 07-1402, MA, USA), phosphoenolpyruvate carboxykinase (PEPCK, Santa Cruz Biotechnology, code sc- 32879), glucose-6-phosphatase (G6Pase, Santa Cruz Biotechnology, code sc-25840, CA, USA), manganese superoxide dismutase (SOD, Santa Cruz Biotechnology, code sc-30080, CA, USA), Catalase (Santa Cruz Biotechnology, code sc-50508, CA, USA), glutathione peroxidase (GPx, Santa Cruz Biotechnology, code sc-133160, CA, USA) and glutathione reductase (GRx, Santa Cruz Biotechnology, code sc-133245, CA, USA). Then, the membranes were washed with T-TBS containing 0.05 % Tween-20 and incubated with specific secondary antibodies for one hour. The structural protein β-actin (Santa Cruz Biotechnology, code sc- 81178, CA, USA) was obtained by stripping the PVDF membrane proteins from the liver and was used to correct the expression of the above-mentioned proteins. The bands were detected via chemiluminescence using an ECL reagent kit (GE Healthcare BioSciences), and images were

obtained using the ChemiDoc system (Bio-Rad, USA). The density of the signals was measured using Image J software, version 1.49c for Windows (Wyne Rasband, National Institutes of Health, USA).

Quantitative real-time PCR

Total RNA was extracted from approximately 50 mg of liver tissue using the TRIzol reagent (Invitrogen, CA, USA). RNA quantification was performed with a NanoVue spectrophotometer (GE Life Sciences), and 1 mg of RNA was treated with DNase I (Invitrogen). The synthesis of first-strand cDNA was performed from mRNA using oligo (dT) and Superscript III Reverse Transcriptase (both Invitrogen). Quantitative real-time PCR (RT-qPCR) used the StepOne Plus Real-Time PCR System (Life Technologies, CA, USA) and SYBR Green mix (Invitrogen). Primers for qPCR were designed using Primer3 software online as indicated in Table 2. Beta-actin was employed to normalize the expression of selected genes. The efficiencies of the RT-qPCR assays for the target and the beta-actin gene were approximately equal and were calculated from a cDNA dilution series. The real-time PCR amplifications were performed as follows: after a pre-denaturation and polymerase activation program (95 min at 4° C), forty-four cycles of 95° C for 10 s and 60° C for 15 seconds were run, followed by a melting curve program (60-95° C with a heating rate of 0.1° C/s). The negative controls consisted of wells in which cDNA was substituted with deionized water. The relative expression ratio (RQ) of mRNA was calculated from the $2^{-\Delta\Delta Ct}$ equation, in which -ΔCT expresses the difference between the number of cycles (CT) for the target genes and beta-actin.

Statistical analysis

In the manuscript, data are expressed as the mean and standard error of the mean. The samples were tested for normality and homogeneity of variances, and differences between the groups were tested via one-way ANOVA with the Holm-Sidak posthoc test (GraphPad Prism v. 6.05 for Windows, San Diego, CA, USA). In all cases, a *P*-value <0.05 was considered statistically significant.

Results

Food intake and body composition

Neither the food intake nor energy intake of the animals showed significant differences during the experiment (data not show). Consequently, BM evolution was not different between the groups (Fig. 1).

The body mass was not different among the groups. However, the ratio IAF/SF was significantly higher in the HFru and HSu groups when compared with the SC ($P<0.05$). In addition, the HSu group showed higher ratio IAF/SF than the HFru group ($P<0.05$) (Fig. 2).

Biochemistry

Most of the data were significantly higher in both Hsu and HFru groups than in the SC group ($P<0.05$) as follows: a) the lipid profile (total cholesterol and triacylglycerol), b) the carbohydrate metabolism (glucose, insulin and HOMA-IR), c) the pro-inflammatory adipokines (resistin and IL-6), d) the plasmatic levels of the leptin and MCP-1. Comparing the HSu group with the HFru group we observed higher values in the Hsu group, even to ALT levels ($P<0.05$). The greater ratio IAF/SF might be an explanation of these findings, at least partially. On the contrary, the adiponectin, an anti-inflammatory adipokine, was lower in both Hsu and HFru groups in comparison with the SC group ($P<0.05$) (Table 3).

Liver

Figure 2 shows the open view of the abdomen of representative animals. In this figure, the liver seems altered, especially in the HFru group, although the liver mass did not show significant differences among the groups: SC (0.98 g ± 0.08 g); HFru (1.28 g ± 0.09 g), and HSu (1.24 g ± 0.09 g).

Nevertheless, the liver of animals in the fructose and sucrose treatment groups exhibited abundant fatty infiltration and some areas of necroinflammation, as illustrated in Fig. 3. Increases in hepatic steatosis of 446 % in the HFru group ($P<0.001$) and 430 % in the HSu group ($P<0.001$) were seen relatively in the SC group.

Protein expression and target genes in the liver

The lipogenesis and gluconeogenesis were increased, and beta-oxidation was decreased together with an antioxidant imbalance in the Hsu and HFru animals compared with the SC group.

The SREBP-1c a transcription factor was increased in both HFru and HSu groups than in the SC group (P<0.001). Synergically, the ChREBP and the PPARgamma were higher in the HFru group (P<0.05) and the HSu group (P<0.01) in comparison with the SC group. Contrarily, the PPARalpha was lower in both HFru and HSu than in the SC group (P<0.05). GLUT-2, PEPCK and G6Pase (involved in gluconeogenesis) were more expressed in both HFru and HSu groups than in the SC group (P<0.05) (Fig. 4). There was a prevalence of genes involved in lipogenesis towards the reduction of beta-oxidation.

There was an imbalance in the oxidative stress with reduced expression of SOD, catalase and GRx in both HSu and HFru groups in comparison with the SC group (P< 0.05), but the GPx expression was not different between the groups (Figs. 5 and 6).

Discussion

The metabolism of carbohydrates and lipids changed in different ways in the animals assessed in the present study. However, increases in total cholesterol, triacylglycerol, and liver enzymes as well as in the inflammatory status of the groups fed diets with a high-fructose and high-sucrose content were found in this work. This is a significant experimental observation because the excessive intake of fructose and sucrose in the human population correlates with the current epidemic of obesity.[15]

The use of fructose as a sweetener for diabetic individuals was thought be beneficial to minimize the impact on blood glucose compared with ordinary sugar.[16] However, medium- and long-term consumption of diets rich in fructose results in hyperglycemia, elevated plasma triacylglycerol levels, inflammation, IR and NAFLD, comparable to the effects associated with sucrose consumption.[17]

Even though in our study animals did not exhibit increased food intake, the adipoinsular axis was dysregulated by the experimental diets, which was verified through hyperleptinemia and hyperinsulinemia. This finding is in accord with results reported in the literature showing that animals subjected to a diet rich in sucrose (32 %) for eight weeks exhibited hyperglycemia, hyperinsulinemia and hyperleptinemia without weight gain.[1]

The MCP-1 is responsible for the activation and infiltration of macrophages in the adipose tissue. MCP-1 usually has increased expression in cases of NAFLD and IR.[18, 19] The macrophages, in turn, are a significant source of tumor necrosis factor (TNF) alpha, and IL-6,[20] and leptin seems to impair the insulin signaling in murine adipocyte.[21] In addition, leptin is suggested to have pro-inflammatory effects.[22] In the current study, we did not observe significant differences in the fatty pads. However, we found the highest ratio IAF/SF in the HSu group, which may explain in part the high plasma levels of leptin and MCP-1 found in the HSu group. Moreover, we found increases in IL-6 and resistin in the plasma and a concomitant reduction of adiponectin in both the HFru and HSu groups.

The adverse potential effect of fructose consumption should be linked to the characteristic hepatic metabolism of fructose and glucose.[23, 24] The metabolism of fructose bypasses the glycolysis, acts as an unregulated source of substrates for lipolysis and regulates the expression of lipogenic genes through induction of SREBP-1c and ChREBP. In addition, it leads to a reduced fatty acid oxidation through downregulation of PPAR-alpha, what explains the ability to generate steatosis.[25] We observed an increased expression (proteins and genes) of SREBP-1c, ChREBP and PPAR-gamma, regulators of lipogenesis, after the intake of sucrose or fructose and the reduction of PPAR-alpha.

The PPAR-gamma activation induces the expression of genes involved in insulin signaling, such as adiponectin, of PEPCK and insulin-2 receptor (IRS-2).[26] PEPCK and G6Pase are critical enzymes in gluconeogenesis and are regulated at the transcriptional level in the liver, being activated by glucagon while fasting and suppressed by insulin after feeding.[27] GLUT2 also plays a role in this process, promoting an influx of glucose in the liver during the postprandial period and its efflux under fasting conditions.[28] The increased glucose production, in response to the increase in G6Pase expression, results in activation of ChREBP and subsequent activation of its target genes, including: ACC, FAS (fatty acid synthase) and L-PK (L-type pyruvate kinase), favoring new fatty acid synthesis.[29] We observed increased

expression of the GLUT-2, PEPCK, and G6Pase in HFru and HSu groups, demonstrating hepatic alterations involved in insulin signaling and carbohydrate metabolism.

ALT is a marker that correlates with liver damage,[30] and we suggested that fructose intake has an impact on this result with increased ALT pronounced when compared to HSu group. In addition, has been suggested that NAFLD may be the most common cause of chronically elevated transaminase levels.[31]

NAFLD-NASH progression may be the consequence of hepatic lipotoxicity caused by excess FFAs, which, in turn, can induce the formation of ROS, resulting in lipotoxic stress in the mitochondria and the endoplasmic reticulum, with consequent dysfunction and cell death occurring via apoptosis or necrosis.[32, 33] In the current study, the fructose and sucrose contributed to increased steatosis with the presence of areas of necroinflammation in the liver, as well an imbalance in ROS that are factors that correlate with the transition from NAFLD to NASH.

NAFLD favors the production of ROS and decreases the synthesis of hepatic antioxidants.[34] The liver is rich in antioxidant defense mechanisms, which involve reduced glutathione (GSH), vitamins C and E, superoxide dismutase (SOD), catalase (CAT), glutathione peroxidase (GPx) and glutathione reductase (GRx), among others.[35] The accumulation of cholesterol plays a role in the induction of mitochondrial oxidative stress through the depletion of GSH in hepatocytes and the formation of pro-inflammatory cytokines.[36] Our study demonstrated that both fructose and sucrose intake had adverse effects on the antioxidant defenses. The hepatocytes exposure to ROS tends to lead to an imbalance in favor of pro-oxidants and/or an imbalance of antioxidant species, culminating in hepatic lesions, as observed in the present study. These findings are in accordance with what was previously demonstrated in rats fed fructose for eight weeks: reduced glucose tolerance, insulin sensitivity, increased AST/ALT, triacylglycerol, and thiobarbituric acid reactive substances.[37]

In a previous study, the effects of a diet rich in sucrose and rich in fructose were different in four strains of mice. However, the sucrose led to more overeating and consequent increased weight gain and adiposity compared to fructose, regardless of the mouse strain.[38] Our findings in the C57BL/6 mice did not find relevant differences in the body mass comparing the animals fed a sucrose-rich diet or a fructose-rich diet.

In the current study, we observed that the mice of the C57BL/6 strain fed a diet rich in sucrose or fructose developed comparable adverse effects on carbohydrate metabolism, proinflammatory profile, antioxidant imbalance, and NAFLD. Consequently, we concluded that there are comparable adverse effects of the diets rich in sucrose or rich in fructose in the mice of the C57BL/6 strain.

References

1. L. S. Oliveira, D. A. Santos, S. Barbosa-da-Silva, C. A. Mandarim-de-Lacerda and M. B. Aguila, *J Nutr Biochem*, 2014, **25**, 193-200.
2. E. E. Aller, I. Abete, A. Astrup, J. A. Martinez and M. A. van Baak, *Nutrients*, 2011, **3**, 341-369.
3. S. P. Murphy and R. K. Johnson, *Am J Clin Nutr*, 2003, **78**, 827S-833S.
4. R. H. Lustig, *J Am Diet Assoc*, 2010, **110**, 1307-1321.
5. Y. Sumida, E. Niki, Y. Naito and T. Yoshikawa, *Free Radic Res*, 2013, **47**, 869-880.
6. A. Takaki, D. Kawai and K. Yamamoto, *International journal of molecular sciences*, 2013, **14**, 20704-20728.
7. Z. Tariq, C. J. Green and L. Hodson, *Liver international: official journal of the International Association for the Study of the Liver*, 2014, **34**, e180-190.
8. Z. H. Yang, H. Miyahara, J. Takeo and M. Katayama, *Diabetol Metab Syndr*, 2012, **4**, 32.
9. E. M. Brunt, C. G. Janney, A. M. Di Bisceglie, B. A. Neuschwander-Tetri and B. R. Bacon, *Am J Gastroenterol*, 1999, **94**, 2467-2474.
10. V. G. Giby and T. A. Ajith, *World journal of hepatology*, 2014, **6**, 570-579.
11. P. G. Reeves, F. H. Nielsen and G. C. Fahey, Jr., *J Nutr*, 1993, **123**, 1939-1951.
12. D. R. Matthews, J. P. Hosker, A. S. Rudenski, B. A. Naylor, D. F. Treacher and R. C. Turner, *Diabetologia*, 1985, **28**, 412-419.
13. M. Catta-Preta, L. S. Mendonca, J. Fraulob-Aquino, M. B. Aguila and C. A. Mandarim-de-Lacerda, *Virchows Arch*, 2011, **459**, 477-485.
14. M. B. Aguila, A. R. Pinheiro, L. B. Parente and C. A. Mandarim-de-Lacerda, *Liver Int*, 2003, **23**, 363-370.
15. R. H. Lustig, L. A. Schmidt and C. D. Brindis, *Nature*, 2012, **482**, 27-29.

16. I. Muraki, F. Imamura, J. E. Manson, F. B. Hu, W. C. Willett, R. M. van Dam and Q. Sun, *BMJ*, 2013, **347**, f5001.
17. E. J. Schaefer, J. A. Gleason and M. L. Dansinger, *J Nutr*, 2009, **139**, 1257S-1262S.
18. H. Kanda, S. Tateya, Y. Tamori, K. Kotani, K. Hiasa, R. Kitazawa, S. Kitazawa, H. Miyachi, S. Maeda, K. Egashira and M. Kasuga, *J Clin Invest*, 2006, **116**, 1494-1505.
19. N. Kamei, K. Tobe, R. Suzuki, M. Ohsugi, T. Watanabe, N. Kubota, N. Ohtsuka-Kowatari, K. Kumagai, K. Sakamoto, M. Kobayashi, T. Yamauchi, K. Ueki, Y. Oishi, S. Nishimura, I. Manabe, H. Hashimoto, Y. Ohnishi, H. Ogata, K. Tokuyama, M. Tsunoda, T. Ide, K. Murakami, R. Nagai and T. Kadowaki, *J Biol Chem*, 2006, **281**, 26602-26614.
20. P. Trayhurn and I. S. Wood, *Br J Nutr*, 2004, **92**, 347-355.
21. G. Muller, J. Ertl, M. Gerl and G. Preibisch, *The Journal of biological chemistry*, 1997, **272**, 10585-10593.
22. G. Paz-Filho, C. Mastronardi, C. B. Franco, K. B. Wang, M. L. Wong and J. Licinio, *Arquivos brasileiros de endocrinologia e metabologia*, 2012, **56**, 597-607.
23. L. Tappy and K. A. Le, *Physiol Rev*, 2010, **90**, 23-46.
24. P. A. Mayes, *Am J Clin Nutr*, 1993, **58**, 754S-765S.
25. K. Nomura and T. Yamanouchi, *J Nutr Biochem*, 2012, **23**, 203-208.
26. L. Guo and R. Tabrizchi, *Pharmacol Ther*, 2006, **111**, 145-173.
27. R. J. Perry, V. T. Samuel, K. F. Petersen and G. I. Shulman, *Nature*, 2014, **510**, 84-91.
28. G. Guillemain, M. Loizeau, M. Pincon-Raymond, J. Girard and A. Leturque, *J Cell Sci*, 2000, **113 (Pt 5)**, 841-847.
29. G. Filhoulaud, S. Guilmeau, R. Dentin, J. Girard and C. Postic, *Trends in endocrinology and metabolism: TEM*, 2013, **24**, 257-268.
30. A. J. Hanley, K. Williams, A. Festa, L. E. Wagenknecht, R. B. D'Agostino, Jr. and S. M. Haffner, *Diabetes*, 2005, **54**, 3140-3147.
31. J. M. Clark, F. L. Brancati and A. M. Diehl, *Am J Gastroenterol*, 2003, **98**, 960-967.
32. H. Malhi and G. J. Gores, *Semin Liver Dis*, 2008, **28**, 360-369.
33. M. Trauner, M. Arrese and M. Wagner, *Biochim Biophys Acta*, 2010, **1801**, 299-310.
34. C. Podrini, M. Borghesan, A. Greco, V. Pazienza, G. Mazzoccoli and M. Vinciguerra, *Curr Pharm Des*, 2013, **19**, 2737-2746.
35. I. A. Leclercq, *Clin Sci (Lond)*, 2004, **106**, 235-237.

36. M. Mari, F. Caballero, A. Colell, A. Morales, J. Caballeria, A. Fernandez, C. Enrich, J. C. Fernandez-Checa and C. Garcia-Ruiz, *Cell metabolism*, 2006, **4**, 185-198.

37. J. D. Botezelli, L. T. Cambri, A. C. Ghezzi, R. A. Dalia, F. A. Voltarelli and M. A. de Mello, *Lipids Health Dis*, 2012, **11**, 78.

38. J. I. Glendinning, L. Breinager, E. Kyrillou, K. Lacuna, R. Rocha and A. Sclafani, *Physiol Behav*, 2010, **101**, 331-343.

Table 1 - Diet Composition. Groups: SC (standard chow), HFru (high-fructose diet) and HSu (high-sucrose diet).

Nutrients (g/Kg)	Groups		
	SC	**HFru**	**Hsu**
Casein	140.0	140.0	140.0
Corn starch	620.692	296.792	296.792
Sucrose	100.0	-	423.9
Fructose	-	423.9	-
Soybean oil	40.0	40.0	40.0
Fiber	50.0	50.0	50.0
Vitamin mix	10.0	10.0	10.0
Mineral mix	35.0	35.0	35.0
Cystine	1.8	1.8	1.8
Coline	2.5	2.5	2.5
Antioxidant	0.008	0.008	0.008
Total (g)	1000.0	1000.0	1000.0
Energy (KJ/kg)	15900	15900	15900
Carbohydrate (%, energy)	76 %	76 %	76 %
• **Sucrose (%, energy)**	10 %	-	45 %
• **Fructose (%, energy)**	-	45 %	-
Protein (%, energy)	14 %	14 %	14 %
Lipids (%, energy)	10 %	10 %	10 %

Table 2 - RT-qPCR primers and respective sequences.

Gene	(5'-3')	Primers
β-actin	FW	TGTTACCAACTGGGACGACA
β-actin	RV	GGGGTGTTGAAGGTCTCAAA
SREBP-1c	FW	AGCAGCCCCTAGAACAAACA
SREBP-1c	RV	TCTGCCTTGATGAAGTGTGG
ChREBP/ MLXIPL	FW	GCATCCTCATCCGACCTTTA
ChREBP/ MLXIPL	RV	GATGCTTGTGGAAGTGCTGA
PPAR-γ	FW	CATCGAGGACATCCAAGACA
PPAR-γ	RV	ACGATCTGCCTGAGGTCTGT
PPAR-α	FW	TCTTCCCAAAGCTCCTTCAA
PPAR-α	RV	TCGGACTCGGTCTTCTTGAT
MNSOD	FW	AACCATCCACTTCGAGCAGA
MNSOD	RV	GGTCTCCAACATGCCTCTCT
CATALASE	FW	ACATGGTCTGGGACTTCTGG
CATALASE	RV	CAAGTTTTTGATGCCCTGGT
GPX-1	FW	GTCCACCGTGTATGCCTTCT
GPX-1	RV	TCTGCAGATCGTTCATCTCG
GRx	FW	CACGACCATGATTCCAGATG
GRx	RV	CAGCATAGACGCCTTTGACA

Abbreviations: ChREBP, Carbohydrate responsive element-binding protein; GPX, glutaredoxin; Glutathione peroxidase; PPAR, peroxisome proliferator-activated receptors; MLXIPL, MLX-interacting protein-like; MNSOD, manganese superoxide dismutase; SREBP, Sterol regulatory element-binding transcription fator.

Table 3 - Plasma biochemical responses. Values are means ± standard error. Symbols represent significant differences from [a] SC and [b] HFru, $P \leq 0.05$, assessed using a one-way ANOVA with post-hoc Holm-Sidak testing. Groups: SC (standard chow), HFru (high-fructose diet) and HSu (high-sucrose diet).

Data	Groups		
	SC	**HFru**	**HSu**
Adiponectin (10^6 pg/ml)	7.1 ± 6.9	4.6 ± 6.6 [a]	4.4 ± 6.9 [a]
ALT (IU/L)	19.8 ± 3.3	45.2 ± 4.2 [a]	31.1 ± 1.8 [a] [b]
AST (IU/L)	42.2 ± 4.9	84.6 ± 7.8 [a]	80.2 ± 9.6 [a]
Glucose (mmol/L)	5.6 ± 0.2	10.3 ± 0.7 [a]	11.0 ± 1.1 [a]
HOMA-IR	5.5 ± 0.9	21.8 ± 4.6 [a]	21.3 ± 3.4 [a]
IL-6 (pg/ml)	6.5 ± 1.5	16.1 ± 1.6 [a]	11.9 ± 1.3 [a]
Insulin (µIU/L)	18.9 ± 3.8	43.8 ± 7.9 [a]	41.0 ± 6.4 [a]
Leptin (10^3pg/ml)	6.1 ± 0.3	9.2 ± 0.9 [a]	15.0 ± 0.9 [a] [b]
MCP-1 (pg/ml)	8.4 ± 0.6	20.1 ± 2.1 [a]	30.1 ± 4.1 [a] [b]
Resistin (10^3 pg/ml)	1.3 ± 0.05	1.8 ± 0.1 [a]	1.7 ± 0.07 [a]
Total cholesterol (mg/dl)	117.6 ± 6.9	164.5 ± 13.1 [a]	159.0 ± 12.3 [a]
Triacylglycerol (mg/dl)	59.4 ± 3.5	75.7 ± 2.8 [a]	76.0 ± 2.7 [a]

Figure legends

Figure 1: Body Mass. The diets were administered for 15 weeks. The presented values are the means ± standard error. Groups: SC (standard chow), HFru (high-fructose diet) and HSu (high-sucrose diet).

Figure 2: Left panel, the open view of the abdomen of representative animals. The yellowish liver is related to the content of intrahepatic fat (steatosis) and is more evident in the HFru group of this panel. Right graph, fat mass distribution (black bar, intra-abdominal fat; white bar, subcutaneous fat). Groups: SC (standard chow), HFru (high-fructose diet) and Hsu (high-sucrose diet). The [a] represents difference from SC, $P<0.05$, assessed using one-way ANOVA with posthoc Holm-Sidak testing.

Figure 3: Volume density of hepatic steatosis. Liver from the (**A**) SC, (**B** and **E**) HFru and (**C** and **F**) HSu groups; (**D**) quantitative measure of steatosis. Increased NAFLD and necroinflammatory areas (arrows) were found in HFru and HSu. There was a significant difference ($P<0.05$) compared with the [a] SC group, assessed using a one-way ANOVA with posthoc Holm-Sidak testing.

Figure 4: (**A**) SREBP-1c; (**B**) ChREBP; (**C**) PPAR-gamma; (**D**) PPAR- α; (**E**) GLUT-2; (**F**) PEPCK and (**G**) G6Pase. For all proteins, expression was normalized to the signal for β-actin (expressed in arbitrary units, a.u); (**H**) representative protein bands of the proteins. The presented values are the means ± standard error. The symbol indicates significant differences from [a] SC, $P<0.05$ assessed using one-way ANOVA with posthoc Holm-Sidak testing.

Figure 5: (**A**) SOD; (**B**) CATALASE; (**C**) GPx; (**D**) GRx. For all proteins, expression was normalized to the signal for β-actin (expressed in arbitrary units, a.u); (**E**) representative protein bands. The presented values are the means ± standard error. The symbol represents significant differences from [a] SC, $P<0.05$ assessed using one-way ANOVA with posthoc Holm-Sidak testing.

Figure 6: (**A**) SREBP-1c; (**B**) ChREBP; (**C**) PPAR-gamma; (**D**) PPAR-alpha; (**E**) SOD; (**F**) Catalase; (**G**) GPx and (**H**) GRx. The endogenous control β-actin was used to normalize the expression of the selected genes. The presented values are the means ± standard error. Symbols

represent significant differences from [a] SC and [b] HFru, $P<0.05$, assessed using one-way ANOVA with posthoc Holm-Sidak testing.

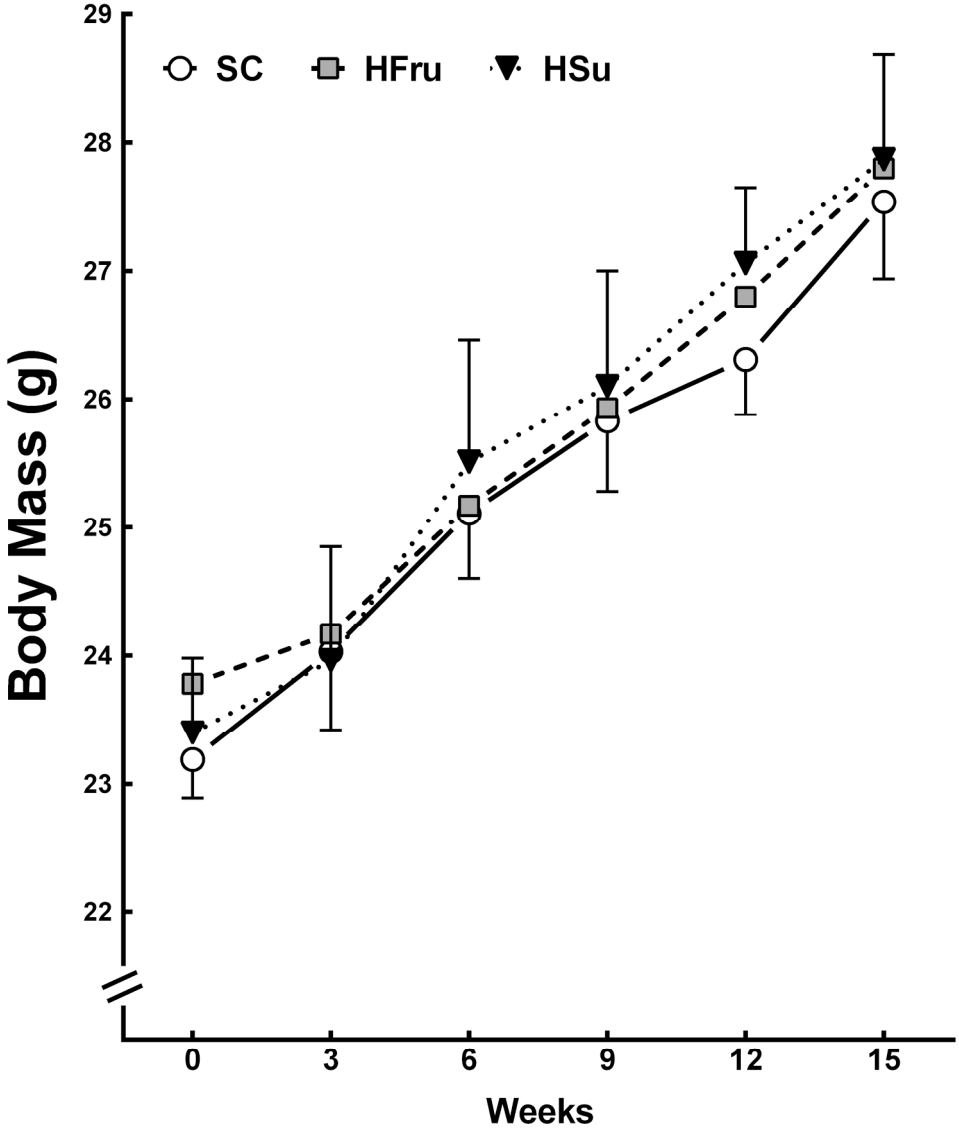

Figure 1: Body Mass. The diets were administered for 15 weeks. The presented values are the means ± standard error. Groups: SC (standard chow), HFru (high-fructose diet) and Hsu (high-sucrose diet).

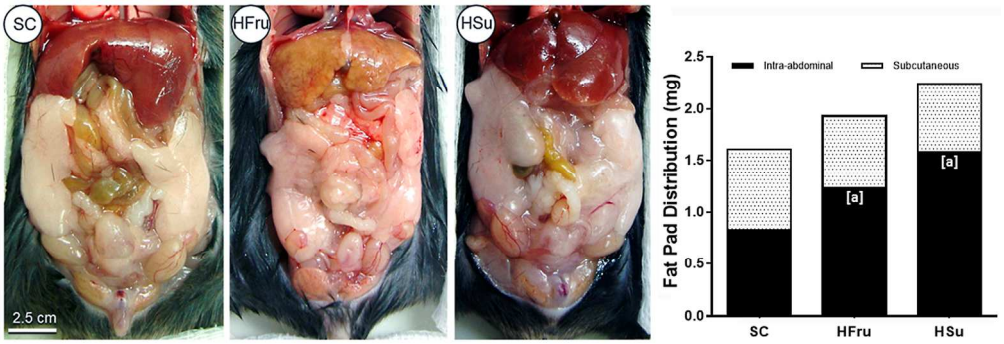

Figure 2: Left panel, the open view of the abdomen of representative animals. The yellowish liver is related to the content of intrahepatic fat (steatosis) and is more evident in the HFru group of this panel. Right graph, fat mass distribution (black bar, intra-abdominal fat; white bar, subcutaneous fat). Groups: SC (standard chow), HFru (high-fructose diet) and Hsu (high-sucrose diet). The [a] represents difference from SC, $P<0.05$, assessed using one-way ANOVA with posthoc Holm-Sidak testing.

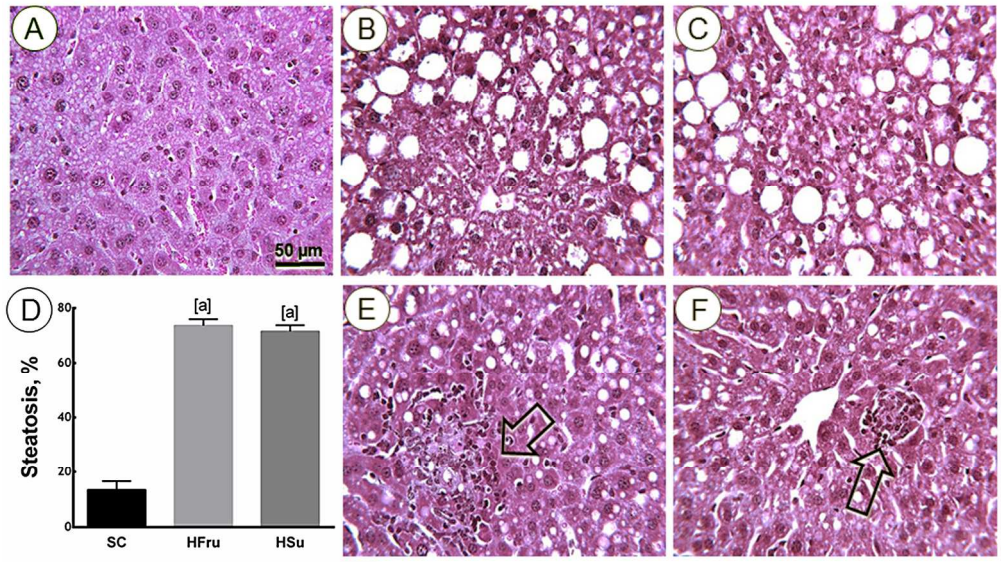

Figure 3: Volume density of hepatic steatosis. Liver from the (A) SC, (B and E) HFru and (C and F) HSu groups; (D) quantitative measure of steatosis. Increased NAFLD and necroinflammatory areas (arrows) were found in HFru and HSu. There was a significant difference ($P<0.05$) compared with the [a] SC group, assessed using a one-way ANOVA with posthoc Holm-Sidak testing.

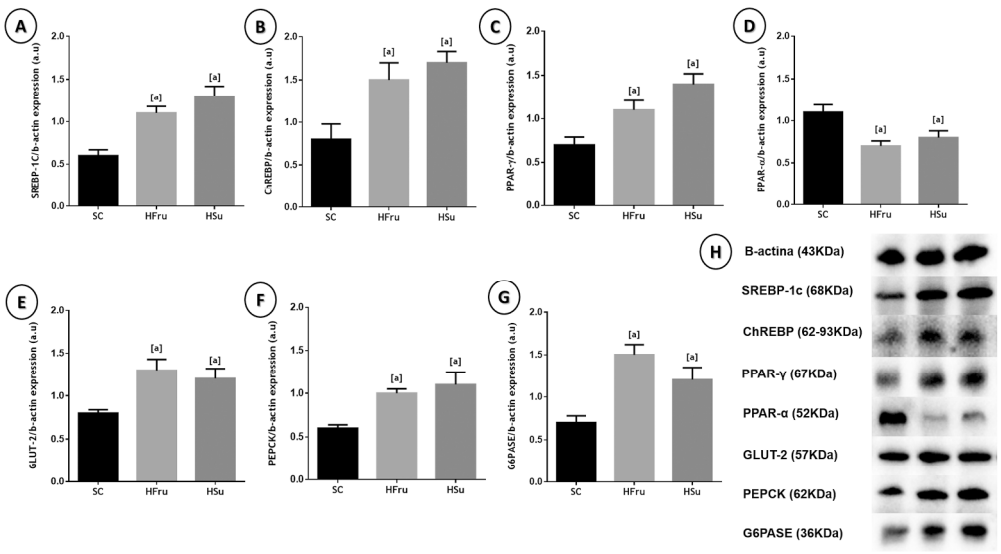

Figure 4: (A) SREBP-1c; (B) ChREBP; (C) PPAR-gamma; (D) PPAR- α; (E) GLUT-2; (F) PEPCK and (G) G6Pase. For all proteins, expression was normalized to the signal for β-actin (expressed in arbitrary units, a.u); (H) representative protein bands of the proteins. The presented values are the means ± standard error. The symbol indicates significant differences from [a] SC, P≤0.05, assessed using one-way ANOVA with post-hoc Holm-Sidak testing.

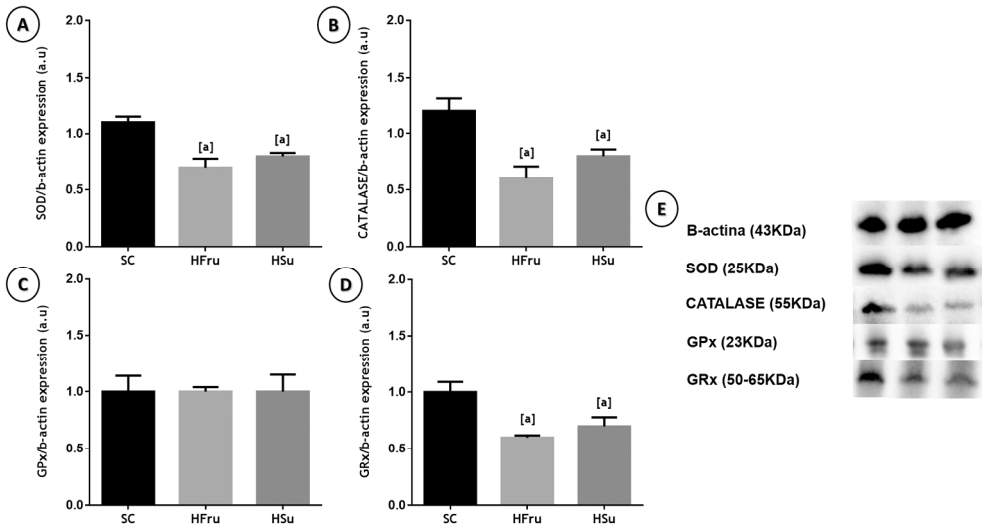

Figure 5: (A) SOD; (B) CATALASE; (C) GPx; (D) GRx. For all proteins, expression was normalized to the signal for β-actin (expressed in arbitrary units, a.u); (E) representative protein bands. The presented values are the means ± standard error. The symbol represents significant differences from [a] SC, P≤0.05, assessed using one-way ANOVA with post-hoc Holm-Sidak testing.

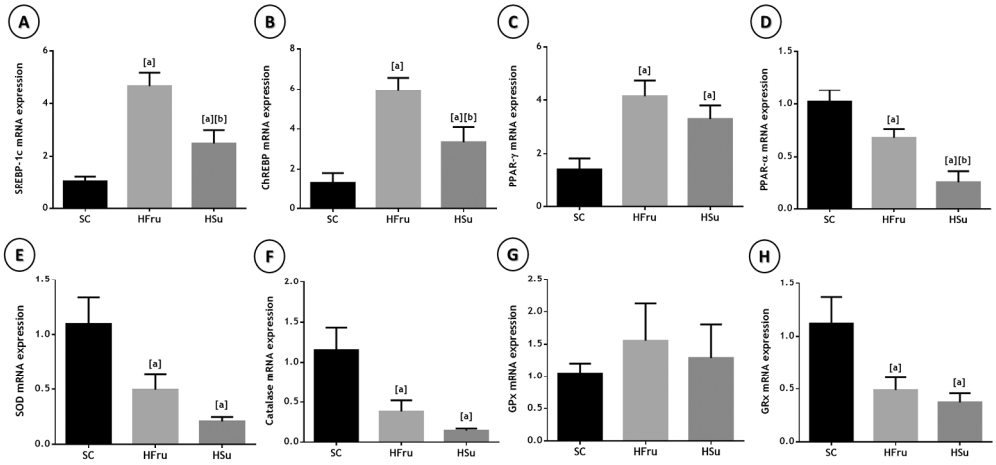

Figure 6: (A) SREBP-1c; (B) ChREBP; (C) PPAR-gamma; (D) PPAR-alpha; (E) SOD; (F) Catalase; (G) GPx and (H) GRx. The endogenous control β-actin was used to normalize the expression of the selected genes. The presented values are the means ± standard error. Symbols represent significant differences from [a] SC and [b] HFru, P≤0.05, assessed using one-way ANOVA with post-hoc Holm-Sidak testing.